Geologica Acta, Vol.4, Nº 4, 2006, 461-469
Available online at www.geologica-acta.com

geologica acta

Exotic accessory minerals in layered chromitites of the Campo Formoso complex (Brazil)

F. ZACCARINI [1] G. GARUTI [2] and R.F. MARTIN [3]

[1] Department of Applied Geological Sciences and Geophysics, University of Leoben
Peter Tunner Str. 5, A 8700 Leoben, Austria, present address:
Instituto Andaluz de Ciencias de la Tierra,
Fuentenueva s/n, 18002, Granada, Spain. E-mail: fedezac@tsc4.com

[2] Dipartimento di Scienze della Terra, University of Modena and Reggio Emilia
Via S. Eufemia 19, 41100 Modena, Italia

[3] Department of Earth and Planetary Sciences, McGill University
3450 University Street, Montréal, Canada H3A 2A7

ABSTRACT

The Campo Formoso stratiform intrusive complex, in Bahia State, Brazil, considered to be of Paleoproterozoic age, consists of a tabular body of ultramafic rocks about 40 km long and 100-1100 m wide. Thick horizons of chromitite are exploited and the deposits are the richest in Brazil. The complex was intruded by the Campo Formoso calc-alkaline batholith, emplaced by the result of the Transamazonian collision-related orogeny. The peridotite was firstly thoroughly serpentinized, then affected by a renewed cycle of hydrothermal alteration as the batholith cooled, leading in the roof zone to emerald mineralization around roof pendants. An even later influx of fluid led to the formation of talc, silica and carbonates, such that the ultramafic rocks were locally converted to listwanite. The chromitite sequences are highly unusual in containing rather exotic minerals, such as monazite-(La), monazite-(Ce), apatite, galena, bismuthinite, antimony, and three unknown minerals of stoichiometry $PbSb_2$, Pb_6Sb and $PbSb_4$, all associated with the clinochlore. The latter phases may have formed during hydrothermal activity in the system Pb-Sb. The presence of these exotic minerals in chromitite, which makes this occurrence unique in the world, strongly support the hypothesis that the La, Ce, P, Pb, Bi and Sb were metasomatically added to the Campo Formoso chromitite horizons by hydrothermal fluids emanating from the nearby Campo Formoso calc-alkaline batholith as it cooled.

KEYWORDS | Campo Formoso. Chromitites. Monazite. Apatite. Pb-S-Sb bearing minerals. Brazil.

INTRODUCTION

The conformable sequences of chromitite of the Campo Formoso layered ultramafic intrusion, in the northern part of the São Francisco craton, Bahia, northeastern Brazil, of Paleoproterozoic age, constitute the main chromium resource in Brazil. They differ from other major occurrences of stratiform chromitite in the world

by the extent of hydrothermal alteration and metasomatic event that have affected the chromian spinel and the enclosing rocks. The original cumulus texture of the ultramafic rocks is generally still recognizable, but no relics of the primary magmatic silicates have survived. The original chromian spinel has fared somewhat better, but in many instances, it was largely transformed to ferrian chromite intimately associated with chromian clinochlore. The reason for this unusual intense alteration of the chromitite horizons has not been addressed in the literature. The development of sophisticated mineralogical analytical techniques now allows us to seek answers in the micro-inclusions of unusual accessory phases, largely in the clinochlore that surrounds the cumulus grains of chromian spinel. In this paper, we document the composition of these neoformed exotic minerals with the aim to understand their genesis and the origin of the fluid phase from which they crystallized.

GEOLOGICAL BACKGROUND

The Campo Formoso layered ultramafic complex is located about 400 km northwest of Salvador, in the State of Bahia (Fig. 1). It forms a tabular, arcuate, monoclinal body approximately 40 km long and 100 to 1100 m wide, and dipping 50°-70° to the southeast (Ferreira et al., 2003). The ultramafic suite rests over Archean granulites of the Carnaíba Group with an age comprised between 2634 ± 19 and 2695 ± 12 Ma (Silva et al., 1997). The upper portion of the layered complex has been removed by erosion; its original thickness is unknown. The ultramafic rocks are also in contact with the Paleoproterozoic Serra de Jacobina Group, dominantly quartzite, and with the Campo Formoso granite (Fig. 1).

The Campo Formoso layered intrusion is well known among economic geologists because it hosts the most prominent chromite deposits of Brazil. At least seven chromitite layers, up to more than 10 m thick, have been discovered in the SW limb of the intrusion, and they have been mined at the localities of Cascabulhos, Pedrinhas, Limoeiro and Mato Limpo (Fig. 1). The chrome ore consists of massive to high-grade disseminated cumulitic chromite, partially to totally transformed into ferrian chromite, in a matrix of altered silicates. Several small veins of quartz cross cut the chromitite layers. The layered intrusion is also of economic interest owing to the development of emerald mineralization where granite-related fluids have interacted with serpentinized peridotite. Emerald mineralization occurs near the northern rim of the Campo Formoso batholith (Fig. 1), but the best-studied occurrences are around the coeval and cogenetic Carnaíba pluton located 20 km to the south. Pegmatite bodies in the cupola of that pluton and nearby K-metasomatized phologopite-bearing serpentinite are the locus of emerald mineralization (Giuliani et al., 1994).

On the basis of K-Ar and $^{40}Ar/^{39}Ar$ measurement on biotite and muscovite, Giuliani et al. (1994) proposed an age of 2032 ± 10 Ma for the first two pulses of the composite granitic batholith. Ages of 2000 Ma and 1911 ± 13 were obtained using the Rb-Sr method (Torquato et al., 1978; Mougeot, 1996). Rudowski (1989) reported a Rb/Sr isochron of 1961 ± 37 Ma, with a $(^{87}Sr/^{86}Sr)_i$ of 0.7065 ± 0.0036. The fluid-circulation events occurred between 1900 and 2000 Ma on the basis of the argon-release spectra proposed by Giuliani et al. (1994), who attributed the overprint of the Transamazonian cycle of activity, i.e., accompanying the cooling of orogenic granite associated with the Transamazonian orogeny.

The dominant rock-type in the batholith is biotite-muscovite granite, locally garnetiferous. The crystals of muscovite attain 3 cm across, and thus the muscovite is largely primary, although texturally it appears to have crystallized near the solidus. The main accessory minerals are apatite, zircon and allanite, the latter associated with a monazite-group mineral. Magnetite is the dominant oxide mineral. Cordierite or possibly sekaninaite $[(Fe,Mg)_2Al_4Si_5O_{18}]$ occurs in the aplitic and pegmatitic segregations. Rudowski (1989) described various types of hydrothermal alteration, for example greisen, K metasomatism leading to "microclinite", pegmatite-aplite dikes, and veins of tourmaline and quartz. Taken at face value, the assemblages of minerals he described and the initial $^{87}Sr/^{86}Sr$ value suggest a calc-alkaline suite and a mixed parentage of I + S source-materials. According to Barbosa and

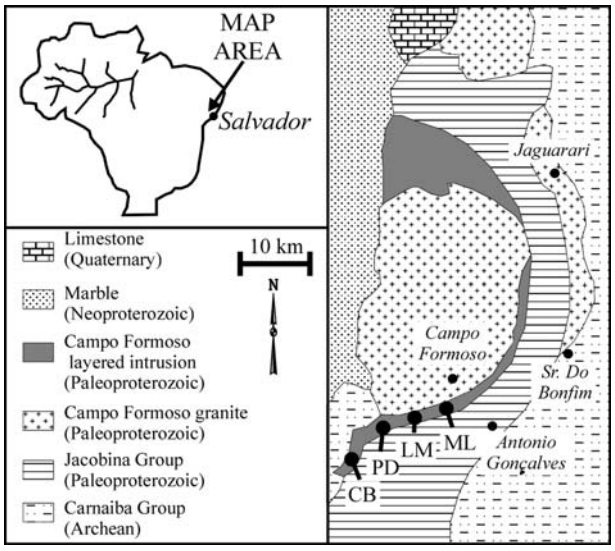

FIGURE 1 | **Geological map of the Campo Formoso area, Bahia, Brazil, showing the location of four chromite mines: Cascabulhos (CB), Pedrinhas (PD), Limoeiro (LM), and Mato Limpo (ML). Modified after de Deus et al. (1982).**

Sabaté (2002), the Campo Formoso batholith and other similar bodies are ultimately the results of the collision of Brazil with Western Africa during the Transamazonian orogeny. Partial melting of an upper mantle in the presence of H_2O and mixing with a magma derived from an amphibolite-facies Archean crustal protolith could well account for the observed peraluminous to metaluminous calc-alkaline suite at Campo Formoso and those documented elsewhere along the Transamazonian orogenic belt (Bastos Leal et al., 2000).

ANALYTICAL PROCEDURES

The accessory minerals were investigated in situ on polished sections using both reflected light and scanning electronic microscopy. We employed a Philips XL-30 instrument at the Inter-department Instrumental Center (CIGS) of the University of Modena and Reggio Emilia, operated with an accelerating voltage of 20-30 kV, and a beam current of 2-10 nA. Quantitative analyses were performed at the Department of Earth Sciences, University of Modena and Reggio Emilia, using an ARL-SEMQ electron microprobe, operated in the WDS mode, at 15-25 kV accelerating voltage, and 15-20 nA beam current with a beam diameter of about 1 μm. The following reference materials were used to analyze the accessory minerals: natural galena, bismuthinite, antimony, monazite, crocoite, fluorite, tugtupite and synthetic glasses composed of ThO_2, ZrO_2, UCoSi, La_2YSi_2, Ce_2YSi_2, NdSi, PrSi. The compositions of chromian spinel and silicates were obtained by the analysis of several grains in each section. Quantitative determinations of proportion of selected elements were calibrated on natural minerals: clinopyroxene, olivine, Mn-bearing olivine, chromite and ilmenite, whereas we used metallic Ni as the reference material for the corresponding element. The proportion of trivalent iron in chromian spinel was calculated assuming stoichiometry. On-line reduction of data calculation, of detection limits and automatic correction of the interferences between various pairs of elements were performed with version 3.63, January 1996, of the Probe software (Donovan and Rivers, 1990).

ALTERATION OF THE CHROMITITES AND ASSOCIATED ROCKS

Owing to deep hydrothermal alteration, the mafic-ultramafic rocks of the layered intrusion were transformed to an assemblage of tremolite, actinolite, serpentine-group minerals, chlorite, carbonate and talc. Besnus et al. (1975), Boukili et al. (1983, 1984) and Calas et al. (1984) have recognized four alteration stages: 1) serpentinization, 2) chloritization, 3) carbonation, and 4) weathering.

During the first stage, the primary ferromagnesian silicates were thoroughly transformed to lizardite and chrysotile, whereas the chromian spinel does not seem to have been significantly affected. The in situ conversion did not disturb the orthocumulus texture (Fig. 2).

In contrast, the second stage of alteration presumably involved more oxygenated and perhaps hotter fluids; these did affect the primary spinel-group minerals, causing conversion of Fe^{2+} to Fe^{3+} from the rim toward the core, in a pseudomorphic process that displaced part of the Cr from the structure. The rim became microporous, and the cavities were filled with chromian clinochlore (up to 7% of Cr_2O_3; see also Boukili et al., 1984). Such clinochlore also formed along the interstices of the chromite orthocumulate. Representative compositions of

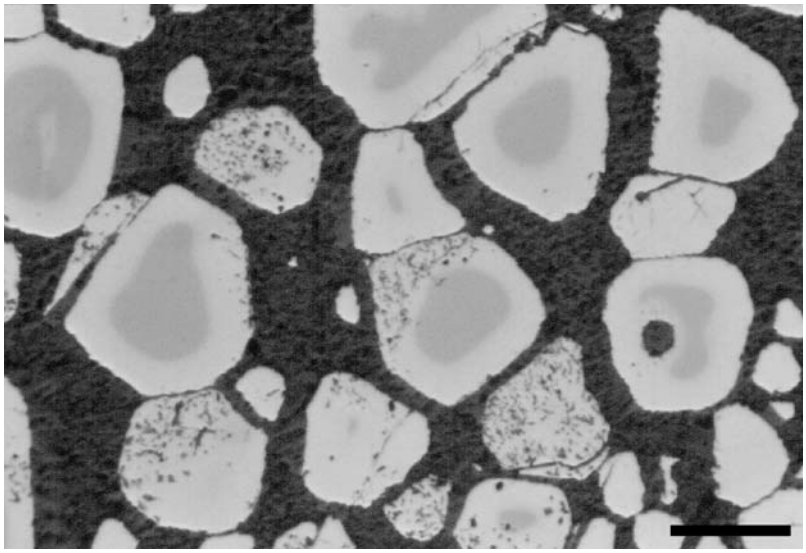

FIGURE 2 **Photos of chromitite from the Campo Formoso layered complex. Preserved orthocumulus texture with a silicate matrix completely transformed to clinochlore. The chromite crystals (dark grey) are partially to totally transformed to ferrian chromite (light grey). Some grains have micropores filled with chromian clinochlore. Reflected light, parallel nicols. Scale bar is 50 μm.**

chromian clinochlore and chromite, including ferrian chromite are listed in Table 1.

There followed a process of carbonation, leading to the conversion of the serpentinized assemblage to one typical of listwanite, consisting of magnesite, stichtite and talc, accompanied by minor dolomite, opal and quartz. The porous spinel grains underwent a further step of alteration that caused a reduction in grain size owing to the net dissolution (Boukili et al., 1983). Finally, the weathering process led to the formation of a laterite cover about 30 m in thickness, composed mainly of smectite-group minerals like volkonskoite and nontronite, along with kaolinite and goethite. Each of these four cycles of fluid-circulation activity seems to have involved fluids of distinct composition, temperature and pH.

CHLORITE GEOTHERMOMETRY

We have used the composition of chlorite as a geothermometer. In addition to the usual words of caution concerning the inherent validity of this approach, we realize that the influence of structurally bound Cr on the equilibria on

TABLE 1 | **Representative electron microprobe compositions of clinochlore and chromite from Campo Formoso layered chromitites.**

Wt%	SiO_2	Al_2O_3	Cr_2O_3	MgO	FeO	Fe_2O_3	TiO_2	MnO	NiO	Totals
Clinochlore										
N.1	32.82	12.73	0.72	34.82	1.51	n.c.	n.a.	n.a.	n.a.	82.60
N.2	34.56	15.09	2.11	31.33	1.93	n.c.	n.a.	n.a.	n.a.	85.02
N.3	31.53	17.23	3.04	33.37	1.89	n.c.	n.a.	n.a.	n.a.	87.06
N.4	33.15	12.43	4.08	33.71	3.11	n.c.	n.a.	n.a.	n.a.	86.48
N.5	33.84	13.2	4.08	35.53	1.08	n.c.	n.a.	n.a.	n.a.	87.73
N.6	33.19	13.97	4.23	34.33	1.44	n.c.	n.a.	n.a.	n.a.	87.16
N.7	33.27	12.18	4.39	34.37	0.97	n.c.	n.a.	n.a.	n.a.	85.18
N.8	32.87	12.79	4.41	34.66	0.9	n.c.	n.a.	n.a.	n.a.	85.63
N.9	32.91	11.84	4.42	33.85	3.12	n.c.	n.a.	n.a.	n.a.	86.14
N.10	33.23	12.2	5.1	34.6	1.55	n.c.	n.a.	n.a.	n.a.	86.68
N.11	30.94	12.62	5.87	32.79	0.74	n.c.	n.a.	n.a.	n.a.	82.96
N.12	29.96	13.52	6.07	32.51	0.91	n.c.	n.a.	n.a.	n.a.	82.97
N.13	32.08	10.21	6.09	34.67	1.03	n.c.	n.a.	n.a.	n.a.	84.08
N.14	31.6	18.13	6.15	33.46	2.48	n.c.	n.a.	n.a.	n.a.	91.82
N.15	32.41	13.21	6.73	34.2	0.86	n.c.	n.a.	n.a.	n.a.	87.41
Unaltered chromite										
N.1	0.20	19.58	42.37	7.61	22.86	6.54	0.30	0.20	0.15	99.81
N.2	0.29	17.13	45.11	7.97	21.94	6.82	0.21	0.37	0.06	99.90
N.3	0.09	14.14	47.15	6.97	22.82	7.85	0.13	0.62	0.02	99.79
N.4	0.09	13.52	49.29	8.79	20.14	7.49	0.19	0.43	0.10	100.04
N.5	0.13	12.71	50.41	9.23	19.22	7.53	0.19	0.47	0.09	99.98
N.6	0.34	13.81	51.13	9.01	19.96	5.23	0.16	0.24	0.14	100.02
N.7	0.07	13.88	52.69	10.99	16.91	4.87	0.17	0.39	0.06	100.03
N.8	0.07	11.56	54.13	9.92	18.04	5.51	0.17	0.50	0.08	99.98
N.9	0.07	13.79	55.05	13.01	13.93	3.70	0.18	0.25	0.08	100.06
N.10	0.06	11.48	57.34	13.04	13.53	4.01	0.18	0.23	0.10	99.97
Ferrian chromite										
N.1	0.26	0.91	37.19	1.86	28.23	30.55	0.40	0.42	0.22	100.04
N.2	0.32	3.51	45.59	5.42	22.91	20.66	0.48	0.75	0.32	99.96
N.3	0.00	5.45	47.79	3.57	26.26	15.54	0.52	0.75	0.18	100.06
N.4	0.00	6.64	48.10	7.63	20.36	15.83	0.62	0.58	0.21	99.97
N.5	0.00	2.06	51.47	6.41	21.57	17.37	0.36	0.59	0.15	99.98
N.6	0.00	4.39	54.13	6.74	21.46	12.19	0.30	0.68	0.16	100.05
N.7	0.31	6.74	53.54	9.49	17.89	11.25	0.41	0.31	0.09	100.03
N.8	0.00	2.58	52.09	5.87	22.21	15.92	0.31	0.87	0.10	99.95
N.9	0.00	5.54	49.86	5.69	22.99	14.59	0.44	0.85	0.12	100.08

n.c.: not calculated; n.a.: not analyzed

which these geothermometers are based has not been studied experimentally. Three chlorite geothermometers consulted (Cathelineau and Nieva, 1985; Kranidiotis and MacLean, 1987; Zang and Fyfe, 1995) give average results in the range 250-200ºC for the second fluid-circulation event (Fig. 3).

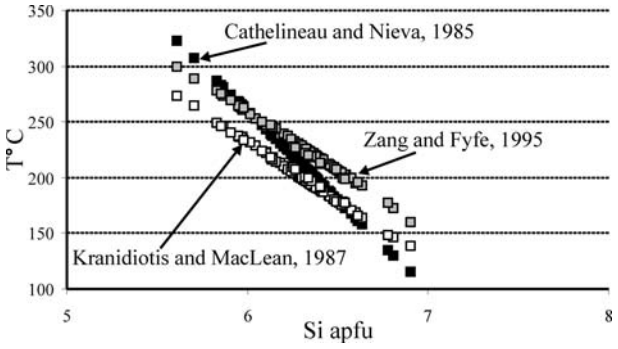

FIGURE 3 | **Results of chlorite geothermometry, based on the formulations of Kranidiotis and MacLean (1987), Cathelineau and Nieva (1985), and Zang and Fyfe (1995).**

THE EXOTIC ACCESSORY MINERALS

Our investigation of the minute grains of accessory minerals developed in layers of chromitite revealed the presence of rather exotic minerals, such as monazite-(La), monazite-(Ce), apatite, galena, bismuthinite, antimony, and unknown Pb-Sb bearing minerals, corresponding to the formula $PbSb_2$, Pb_6Sb and $PbSb_4$. All these minerals are restricted to the secondary silicates of the matrix and to fractures crossing altered chromite grains. Also, they are typically associated with chromian clinochlore and thus seem to have been deposited during the second of the fluid-circulation events.

Monazite-(La) and Monazite-(Ce)

To the best of our knowledge, monazite-group minerals have been never documented in chromitite. More than 50 grains of monazite-(La) and monazite-(Ce) have been recognized in sections studied by scanning electron microscopy. Monazite-(La) occurs as single phase grains, variable in size from 5 up to more than 100 μm, with an irregular shape (Fig. 4). In some cases, grains of monazite contain small inclusions of chromian clinochlore (Fig. 4A). Electron microprobe data (Table 2) show that the compositions of monazite-(La) straddle the boundary between monazite-(La) and monazite-(Ce) (Fig. 5). These grains also contain minor amounts of Pr (up to 2.74 wt% Pr_2O_3), Nd (up to 4.49 wt% Nd_2O_3) and Th (up to 0.64 wt% ThO_2).

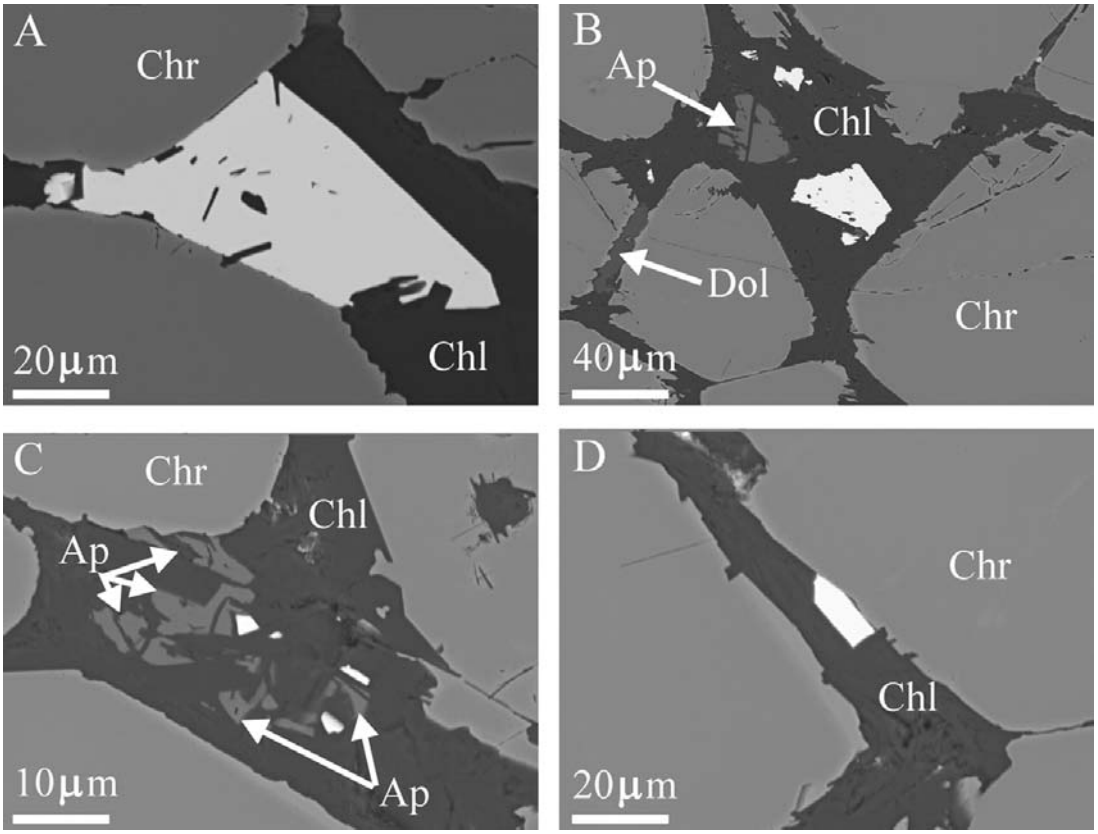

FIGURE 4 | **Back-scattered-electron (BSE) images of monazite-group minerals, either monazite-(La) or monazite-Ce (white grains) associated with clinochlore and chromian spinel in chromitite from Campo Formoso. Symbols: Chr: chromite; Chl: chromian clinochlore; Ap: apatite; Dol: dolomite.**

TABLE 2 | **Representative electron microprobe compositions of monazite from Campo Formoso layered chromitites.**

d.l.	0.05				0.23	0.22	0.03	0.10	0.10	0.03	0.10	
Wt%	CaO	P_2O_5	La_2O_3	Ce_2O_3	Pr_2O_3	Nd_2O_3	UO_2	ThO_2	PbO	ZrO_2	Y_2O_3	Totals
N.1	0.10	28.46	26.94	37.83	0.96	3.78	b.d.l.	0.48	b.d.l.	b.d.l.	0.14	98.69
N.2	0.05	30.16	31.43	33.12	2.10	3.55	b.d.l.	0.52	b.d.l.	b.d.l.	0.22	101.13
N.3	0.05	28.79	31.21	33.10	2.41	3.34	b.d.l.	0.37	b.d.l.	b.d.l.	b.d.l.	99.27
N.4	b.d.l.	29.82	29.82	32.15	2.66	3.68	b.d.l.	0.47	b.d.l.	b.d.l.	b.d.l.	98.59
N.5	0.08	29.33	31.54	31.68	1.56	3.54	b.d.l.	0.50	b.d.l.	b.d.l.	b.d.l.	98.23
N.6	0.09	31.65	30.83	29.92	1.62	3.82	b.d.l.	0.41	b.d.l.	b.d.l.	b.d.l.	98.33
N.7	b.d.l.	29.40	33.09	30.90	2.22	3.79	b.d.l.	0.47	b.d.l.	b.d.l.	b.d.l.	99.87
N.8	b.d.l.	29.91	31.58	30.87	2.16	3.62	b.d.l.	0.51	b.d.l.	b.d.l.	b.d.l.	98.64
N.9	0.11	32.10	32.02	28.40	2.05	3.39	b.d.l.	0.52	b.d.l.	b.d.l.	b.d.l.	98.60
N.10	0.09	29.94	29.92	31.42	2.15	3.64	b.d.l.	0.54	b.d.l.	b.d.l.	b.d.l.	97.69
N.11	0.11	28.74	31.79	31.42	0.82	3.51	b.d.l.	0.51	b.d.l.	b.d.l.	b.d.l.	96.89
N.12	0.13	28.89	30.51	31.90	2.39	3.51	b.d.l.	0.61	b.d.l.	b.d.l.	b.d.l.	97.95
N.13	0.06	28.88	31.66	31.93	1.92	3.41	b.d.l.	0.48	b.d.l.	b.d.l.	b.d.l.	98.34
N.14	0.11	29.03	31.76	33.75	1.92	4.09	b.d.l.	0.52	b.d.l.	b.d.l.	b.d.l.	101.17
N.15	0.11	29.74	32.64	32.95	1.98	3.72	b.d.l.	0.44	b.d.l.	b.d.l.	b.d.l.	101.57
N.16	0.48	27.20	31.81	35.22	0.41	4.09	b.d.l.	0.65	b.d.l.	b.d.l.	b.d.l.	99.86
N.17	0.07	28.66	28.83	33.36	2.74	4.28	b.d.l.	0.50	b.d.l.	b.d.l.	b.d.l.	98.44
N.18	b.d.l.	29.18	32.07	31.84	1.70	3.69	b.d.l.	0.35	b.d.l.	b.d.l.	b.d.l.	98.83
N.19	0.09	28.53	32.06	33.41	1.36	4.49	b.d.l.	0.64	b.d.l.	b.d.l.	0.12	100.71
N.20	b.d.l.	26.26	35.44	33.66	1.19	3.09	b.d.l.	0.44	b.d.l.	b.d.l.	b.d.l.	100.09
At%	Ca	P	La	Ce	Pr	Nd	U	Th	Pb	Zr	Y	
N.1	0.06	14.90	9.34	8.57	0.22	0.84	b.d.l.	0.07	b.d.l.	b.d.l.	0.05	
N.2	0.04	16.53	7.50	7.85	0.50	0.82	b.d.l.	0.08	b.d.l.	b.d.l.	0.08	
N.3	0.04	16.26	7.68	8.08	0.59	0.79	b.d.l.	0.06	b.d.l.	b.d.l.	b.d.l.	
N.4	b.d.l.	16.68	7.27	7.78	0.64	0.87	b.d.l.	0.07	b.d.l.	b.d.l.	b.d.l.	
N.5	0.06	16.54	7.75	7.73	0.38	0.84	b.d.l.	0.08	b.d.l.	b.d.l.	b.d.l.	
N.6	0.06	17.29	7.33	7.07	0.38	0.88	b.d.l.	0.06	b.d.l.	b.d.l.	b.d.l.	
N.7	b.d.l.	16.40	8.04	7.46	0.53	0.89	b.d.l.	0.07	b.d.l.	b.d.l.	b.d.l.	
N.8	b.d.l.	16.69	7.68	7.45	0.52	0.85	b.d.l.	0.08	b.d.l.	b.d.l.	b.d.l.	
N.9	0.08	17.40	7.56	6.66	0.48	0.78	b.d.l.	0.08	b.d.l.	b.d.l.	b.d.l.	
N.10	0.07	16.80	7.31	7.62	0.52	0.86	b.d.l.	0.08	b.d.l.	b.d.l.	b.d.l.	
N.11	0.08	16.48	7.94	7.79	0.20	0.85	b.d.l.	0.08	b.d.l.	b.d.l.	b.d.l.	
N.12	0.10	16.42	7.55	7.84	0.59	0.84	b.d.l.	0.09	b.d.l.	b.d.l.	b.d.l.	
N.13	0.04	16.37	7.82	7.83	0.47	0.82	b.d.l.	0.07	b.d.l.	b.d.l.	b.d.l.	
N.14	0.08	16.15	7.70	8.12	0.46	0.96	b.d.l.	0.08	b.d.l.	b.d.l.	b.d.l.	
N.15	0.08	16.34	7.81	7.83	0.47	0.86	b.d.l.	0.07	b.d.l.	b.d.l.	b.d.l.	
N.16	0.35	15.59	7.94	8.73	0.10	0.99	b.d.l.	0.10	b.d.l.	b.d.l.	b.d.l.	
N.17	0.05	16.30	7.14	8.20	0.67	1.03	b.d.l.	0.08	b.d.l.	b.d.l.	b.d.l.	
N.18	b.d.l.	16.44	7.87	7.76	0.41	0.88	b.d.l.	0.05	b.d.l.	b.d.l.	b.d.l.	
N.19	0.06	16.03	7.85	8.12	0.33	1.07	b.d.l.	0.10	b.d.l.	b.d.l.	0.04	
N.20	b.d.l.	15.27	8.98	8.46	0.30	0.76	b.d.l.	0.07	b.d.l.	b.d.l.	b.d.l.	

d.l.: detection limit; b.d.l.: below detection limit.

In most cases, the levels of concentration of U, Pb and Zr are below the limit of detection of electron microprobe analyses (Table 2). As a result, we were unable to obtain geochronological data concerning the second episode of alteration at the Campo Formoso based on the levels of concentration of U, Pb and Th in the monazite-group minerals.

Apatite

Apatite is a very widely distributed accessory mineral, in a broad array of lithological associations. Despite of its abundance, however, it has never been reported to be associated with chromitite horizons. Apatite, with low F content (less than 0.73 wt%) and relatively high content

of Cl (up to 1.11 wt%) was reported from the metasomatic chromitites of the Finero complex of the Italian Western Alps (Zaccarini et al., 2004). The metasomatic activity in that case seems to have occurred in a region of the mantle undergoing rifting and marked by carbothermal activity. The apatite-group mineral associated with chromitite in the Campo Formoso suite also has possibly a metasomatic origin, but the source of the fluid phase in this case presumably was the Campo Formoso batholith, since Rudowski (1989) has documented the presence of apatite throughout the batholith. The 56 samples of granite analyzed contain between 0.02 and 0.22 wt% P_2O_5 and up to 2650 ppm fluorine.

Pb-S-Sb bearing minerals

A suite of Pb-S-Sb bearing minerals has been encountered in and around grains of chromian spinel. On the basis of results of the chemical analyses (Table 3), we have grouped them as galena, bismuthinite, antimony, and unknown Pb-Sb bearing minerals. Galena forms crystals from 3 up to 50 μm in size (Fig. 6), either as single phase crystals (Fig. 6A) or associated with pentlandite (Fig. 6B). The minerals in the system Pb-Sb have been found as single phase grains, attaining only a few μm across. The compositional data (Table 3) correspond to the stoichiometry $PbSb_2$, Pb_6Sb, $PbSb_4$, and do not match any known species. They, thus, potentially represent new mineral species, but it was not possible to extend the investigation because of the small size of the grains.

From the point of view of phase equilibria, lead is known to melt at 327ºC, and the addition of Sb lowers the freezing point to 247ºC. Thus, it is theoretically possible that the lead-antimony alloys and the antimony in our assemblage crystallized from globules of melt during the hydrothermal stage concomitantly with the growth of the chromian clinochlore. However, the phase diagram illustrated in the metallurgical literatures is that of a simple binary system without solid solution and without binary compounds.

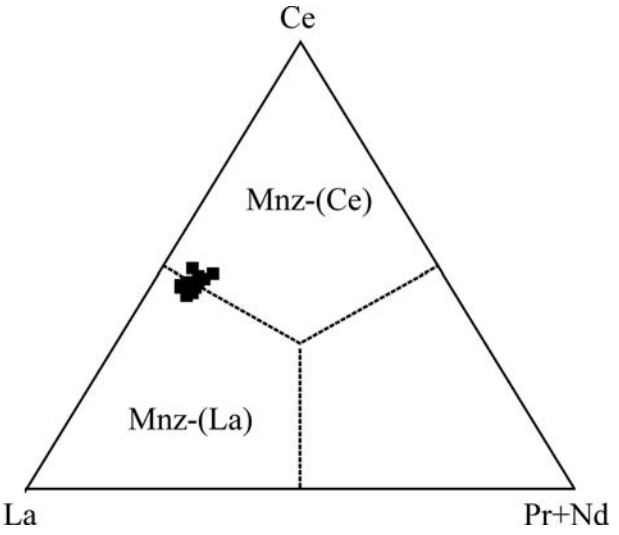

FIGURE 5 | **The proportion of La, Ce, and (Pr + Nd), in at%, in the monazite-group minerals found embedded in clinochlore between grains of chromian spinel from the Campo Formoso layered chromitite. Mnz-(La): monazite-(La), Mnz-(Ce): monazite-(Ce).**

DISCUSSION: PETROGENETIC SIGNIFICANCE OF THE ACCESSORY MINERALS IN THE CAMPO FORMOSO LAYERED CHROMITITES

The presence of exotic minerals such as monazite-(La), monazite e–(Ce), apatite, galena, bismuthinite, antimony, and unknown minerals belonging to the binary system Pb-Sb in chromitite horizons at Campo Formoso strongly supports the hypothesis that the necessary La,

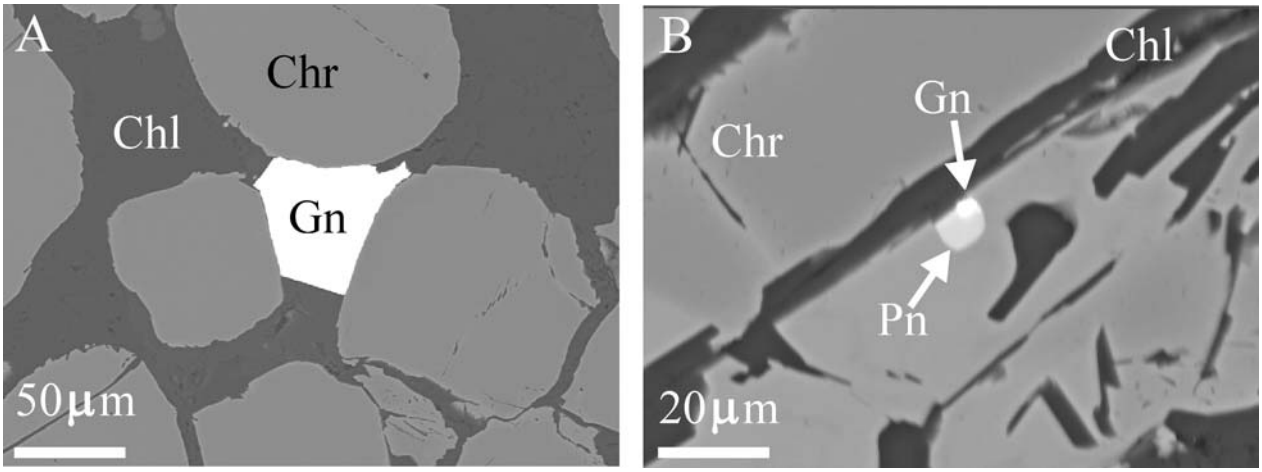

FIGURE 6 | **BSE images of galena found in chromitite at Campo Formoso. Symbols: Gn: galena; Pn: pentlandite; Chr: chromite; Chl: chromian clinochlore.**

TABLE 3 | **Representative electron microprobe compositions of Pb-Sb-Bi minerals from the Campo Formoso layered chromitites.**

Wt%	Pb	S	Sb	Bi	Totals
Bismuthinite					
N.1	1.27	17.08	0.70	81.59	100.64
Antimony					
N.2	1.05		100.00		101.05
N.3	1.51		98.45		99.96
N.4	5.67		94.01	0.28	99.96
Unknown $PbSb_2$					
N.5	45.96		52.57	1.15	99.68
Unknown Pb_6Sb					
N.6	86.81		8.61	0.94	96.36
Unknown $PbSb_4$					
N.7	32.89		68.75	0.46	102.10
N.8	31.85		67.96	1.00	100.81
At%	Pb	S	Sb	Bi	
Bismuthinite					
N.1	0.66	56.97	0.62	41.75	
Antimony					
N.2	0.61	0.00	99.39	0.00	
N.3	0.89	0.00	99.11	0.00	
N.4	3.42	0.00	96.42	0.17	
Unknown $PbSb_2$					
N.5	33.65	0.00	65.51	0.84	
Unknown Pb_6Sb					
N.6	84.78	0.00	14.31	0.91	
Unknown $PbSb_4$					
N.7	21.88	0.00	77.82	0.30	
N.8	21.45	0.00	77.88	0.67	
a.p.f.u	Pb	S	Sb	Bi	
Bismuthinite					
N.1	0.03	2.85	0.03	2.09	
Antimony					
N.2	0.01	0.00	0.99	0.00	
N.3	0.01	0.00	0.99	0.00	
N.4	0.03	0.00	0.96	0.00	
Unknown $PbSb_2$					
N.5	1.01	0.00	1.97	0.03	
Unknown Pb_6Sb					
N.6	5.93	0.00	1.00	0.06	
Unknown $PbSb_4$					
N.7	1.09	0.00	3.89	0.02	
N.8	1.07	0.00	3.89	0.03	

Ce, Nd, Pr, F, Pb and Sb were supplied by the hydrothermal solution emanating from the adjacent batholith as it cooled. Rudowski (1989) has shown that where the activity of such a fluid phase was focused, in cupola environments, Al, K, Si, F, Fe, Rb, Cs, Li, La, Nb, Be, P, Y and Mn were added to serpentinite roof-pendants, leading to their metasomatic conversion to phlogopite, locally emerald-bearing. Of these elements, the availability of K, Rb and Cs is likely a reflection of the hydrothermal Na-for-K ion-exchange affecting microcline, leading to albitized rocks documented to be present in the cupola environment at Campo Formoso. Lead generally also is present in the K site in K-feldspar, and thus can also be expected to have been released during Na-for-K ion-exchange reaction, as Pb is too large cation to be accommodated in the resulting albite. Bismutocolumbite [$Bi(Nb,Ta)O_4$], stibiocolumbite $SbNbO_4$, or stibiobetafite [$(Sb,Ca)_2(Ti,Nb,Ta)_2(O,OH)_7$] are examples of Bi- and Sb-rich phases that could be encountered in occurrences of granitic pegmatite in the batholith, and their destabilization could explain the availability of Bi and Sb in a fluid phase.

The aqueous fluids circulating in the batholith were locally more strongly acid, and caused the total destabilization of alkali feldspar in greisen veins (Rudowski, 1989). Such fluids can be expected to destabilize apatite (e.g., Stoffregen and Alpers, 1987) and monazite-(Ce) (Ayers et al., 2004) in the batholith, leading to the release and mobilization of the light rare-elements and phosphate that led to the monazite-group minerals in the chromitite horizons. The fact that the proportion of La is subequal to that of Ce, and even marginally exceeds that of Ce in some cases, probably reflects the fact that fractionation has occurred as the fluid migrated from the granitic source into peridotite, some of the Ce being incorporated in the earlier-formed monazite lining channelways and fissures along the way. The presence of monazite-(La), a rarely encountered mineral, possibly provides a hint that the chromitite horizons sampled lie in a distal part of a hydrothermal circulating cell set up around the batholith. As an alternative hypothesis to be tested, acidic fluids may have caused the destabilization of the primary phosphates at a much later stage, during the weathering cycle, the final stage of fluid circulation identified by Boukili et al. (1983) and Calas et al. (1984).

ACKNOWLEDGEMENTS

We thank Dr. Maria de Lourdes da Silva Rosa, of the Universidade Federal da Bahia, in Salvador, for sending us the doctoral thesis of Luc Rudowski. RFM acknowledges the continuing support of the Natural Sciences and Engineering Research Council of Canada. F.Z. is grateful to the Austrian Science Fund (FWF Lise Meitner fellowship) for the possibility to spend two years at the University of Leoben. This manuscript has greatly benefited from the constructive criticisms and useful suggestions of the referees Rosario Lunar and Joan Carles Melgarejo, as well as from the associate editor Joaquin Proenza.

REFERENCES

Ayers, J.C., Loflin, M., Miller, C.F., Barton, M.D., Coath, C., 2004. Dating fluid infiltration using monazite. In: Wanty, R.B., Seal II, R.R. (eds.). Eleventh International Symposium on Water-Rock Interaction, Rotterdam, Balkema Publishers, Proceedings, 1, 247-251.

Barbosa, J.S.F., Sabaté, P., 2002. Geological features and the Paleoproterozoic collison of four Archean crustal segments of the Sao Francisco Craton, Bahia, Brazil. A synthesis. Annual Brazilian Academy Sciences, 74, 343-359.

Bastos Leal, L.R., Teixtera, W., Cunha, J.C., de Mendez Leal, A.B., Macambira, M.J.B, da Silva Rosa, M.de L., 2000. Isotopic signatures of Paleoproterozoic granitoids of the Gavião block and implication for the evolution of the São Francisco craton, Bahia, Brazil. Revista Brasiliana Geociências, 30, 66-69.

Besnus, Y., Fusil, G., Janot, C., Pinta, M., Sieffermann, G., 1975. Characteristics of some weathering products of chromitic ultrabasic rocks in Bahia State, Brazil: nontronites, chlorite and chromiferous talc. International Clay Conference, Wilmette, Illinois. Applied Publishing Ltd., Proceedings, 27-34.

Boukili, H., Novikoff, A., Besnus, Y., Soubies, F., Queiroz, C., 1983. Pétrologie des produits de l'altération des roches ultrabasiques à chromite de Campo Formoso, état de Bahia, Brésil. Science Géologique Mémories, 72, 19-28.

Boukili, H., Novikoff, A., Franca, J., 1984. Minéralogie et géochimie des chlorites et hydroxycarbonates chromifères de Campo Formoso, Bahia, Brésil. Cahiers O.R.S.T.O.M. Série Géologique, 16, 141-152.

Calas, G., Manceau, A., Novikoff, A., Boukili, H., 1984. Comportement du chrome dans les minéraux d'alteration du gisement de Campo Formoso (Bahia, Brésil). Bulletin Minéralogie, 107, 755-766.

Cathelineau, M., Nieva, D., 1985. A chlorite solid solution geothermometer. The Los Azufres (Mexico) geothermal system. Contributions to Mineralogy Petrology, 91, 235-244.

de Deus, P.B., d'El Rey, L.J.H., Hasui, Y., Lima e Silva, F., Mandetta, P., de Oliveira, J.G., Franke, N.D., Carvalho, P.R., de Moraes, J.A.C., Miola, W., Vianna, J.S., Duarte, P.M., Qeiroz, W.A., 1982. Caraíba, Pedrinhas and Andorinhas minas, Bahia State: copper and chrome in Archean and/or Proterozoic rocks. International Symposium on Archean and Early Proterozoic geological evolution and metallogenesis, Salvador, Brazil, Abstracts and Excursions, 89-117.

Donovan, J.J., Rivers, M.L., 1990. PRSUPR- a PC based automation and analyses software package for wavelength dispersive electron beam microanalyses. Microbeam Analysis, 66-68.

Ferreira, F.J.F., Almeida Filho, R., da Silva, F.V., 2003. Modelagem de dados aeromagnéticos para estimar largura e espessura do complexo mafico/ultramafico de Campo Formoso-BA. Boletim Paranaense de Geociências, 52, 41-47.

Giuliani, G., Zimmermann, J.L., Montigny, R., 1994. Ar and $^{40}Ar/^{39}Ar$ evidence for a Transamazonian Age (2030-1970 Ma) for the granites and emerald-bearing K-metasomatites from Campo-Formoso and Carnaiba (Bahia, Brazil). Journal of South American Earth Sciences, 7, 149-165.

Kranidiotis, P., MacLean, W.H., 1987. Systematics of chlorite alteration at the Phelps Dodge massive sulfide deposit, Matagami, Quebec. Economic Geology, 82, 1898-1911.

Mougeot, R., 1996. Étude de la limite Archéen-Proterozoic et des mineralizations de Au, U associées: Exemples de la Region de Jacobina (Etat de Bahia, Brésil) et de Carajás (Etat de Pará, Brésil). Doctoral Thesis. University of Montpellier, France.

Rudowski, L., 1989. Pétrologie et géochimie des granites transamazoniens de Campo Formoso et Carnaíba (Bahia, Brasil), et des phlogopitites à émeraudes associées. Doctoral Thesis. University of Paris VI, France.

Silva, L.C., McNaughton, N.J., Melo, R.C., Fletcher, I.R., 1997. U-Pb SHRIMP ages in the Itabuna-Caraíba TTG high-grade Complex: the first window beyond the Paleoproterozoic overprint of the eastern Jequié Craton, NE Brazil. International Symposium on Granites and Associated Mineralization. Salvador, Brazil, Abstracts, 1, 282-283.

Stoffregen, R.E., Alpers, C.N., 1987. Woodhouseite and svanbergite in hydrothermal ore deposits: products of apatite destruction during advanced argillic alteration. The Canadian Mineralogist, 25, 201-211.

Torquato, J.R., Farias Tanner de Oliveira, M.A., Bartels, R.L., 1978. Idade radiométrica do granito de Campo Formoso, BA, uma idade minima para o grupo Jacobina. Revista Brasileira Geociências, 8, 171-179.

Zaccarini, F., Stumpfl, E.F., Garuti, G., 2004. Zirconolite and Zr-Th-U minerals in chromitites of the Finero complex, Western Alps, Italy: evidence for carbonatite-type metasomatism in a subcontinental mantle plume. The Canadian Mineralogist, 42, 1825-1845.

Zang, W., Fyfe, W.S., 1995. Chloritization of the hydrothermally altered bedrocks at the Igarape Bahia gold deposit, Crajas, Brazil. Mineralium Deposita, 30, 30-38.

Manuscript received March 2006;
revision accepted August 2006.